Published in final edited form as:
Neuroimage. 2012 February 1; 59(3): 2504–2510. doi:10.1016/j.neuroimage.2011.08.097.

Examining Cortical Dynamics and Connectivity with Simultaneous Single-Pulse Transcranial Magnetic Stimulation and Fast Optical Imaging

Nathan A. Parks[1], **Edward L. Maclin**[1], **Kathy A. Low**[1], **Diane M. Beck**[1,2], **Monica Fabiani**[1,2], and **Gabriele Gratton**[1,2]

[1]Beckman Institute, University of Illinois Urbana-Champaign

[2]Department of Psychology, University of Illinois Urbana-Champaign

Abstract

Transcranial magnetic stimulation (TMS) is a widely used experimental and clinical technique that directly induces activity in human cortex using magnetic fields. However, the neural mechanisms of TMS-induced activity are not well understood. Here, we introduce a novel method of imaging TMS-evoked activity using a non-invasive fast optical imaging tool, the event-related optical signal (EROS). EROS measures changes in the scattering of near-infrared light that occur synchronously with electrical activity in cortical tissue. EROS has good temporal and spatial resolution, allowing the dynamics and spatial spread of a TMS pulse to be measured. We used EROS to monitor activity induced in primary motor cortex (M1) by a TMS pulse. Left- and right-hand representations were mapped using standard TMS procedures. Optical sources and detectors mounted on thin rubber patches were then centered on M1 hand representations. EROS was recorded bilaterally from motor cortex while unilateral TMS was simultaneously delivered. Robust ipsilateral EROS activations were apparent within 16 ms of a pulse for TMS delivered to both left and right hemispheres. Clear motor evoked potentials (MEPs) were also elicited by these TMS pulses. Movement artifacts could be excluded as a source of EROS, as no activation was present on short-distance optical channels. For left hemisphere TMS subsequent (40 ms) contralateral activity was also present, presumably due to trans-synaptic propagation of TMS-evoked activity. Results demonstrate that concurrent TMS/EROS is a viable and potentially powerful method for studying TMS-induced activity in the human brain. With further development, this technique may be applied more broadly in the study of the dynamics of causal cortico-cortical connectivity.

Keywords

Transcranial Magnetic Stimulation (TMS); the event-related optical signal (EROS); motor evoked potential (MEP); primary motor cortex (M1); connectivity

Transcranial magnetic stimulation (TMS) is becoming an increasingly popular experimental and clinical tool. However, there remains considerable uncertainty regarding the mechanisms through which TMS pulses activate underlying neural tissue, the duration over

which this activity persists, and the extent to which this activity spreads locally and inter-regionally. TMS-evoked activity has been measured in the human brain using several noninvasive neuroimaging techniques (i.e., electroencephalography, EEG, event-related brain potentials, ERPs, functional magnetic resonance imaging, fMRI, positron emission tomography, PET, and functional near-infrared spectroscopy, fNIRS). However, these methods pose significant challenges due to competing electrical or magnetic fields and suffer from either temporal or spatial limitations. The event-related optical signal (EROS; Gratton, Corballis, Cho, Fabiani, & Hood, 1995; Gratton & Fabiani, 2007; 2010), in contrast, has both high spatial and temporal resolution and the optical nature of the signal makes it well suited for use with the strong magnetic fields produced by TMS. Here we demonstrate the efficacy of using EROS to measure the effects of TMS on the human cortex.

TMS is a technique that uses a very strong magnetic field (applied at the scalp) to induce electrical activity in underlying cortical neural tissue. TMS is most often administered as an isolated pulse (single-pulse TMS, or sTMS) or as a series of consecutive pulses (repetitive TMS, or rTMS). STMS transiently activates a particular cortical region for a brief period whereas rTMS continuously stimulates a targeted cortical area and can induce states of cortical depression that outlast the duration of rTMS application (Ziemann, 2004; Huang, Edwards, Rounis, Bhatia, & Rothwell, 2005). In the cognitive neurosciences, sTMS and rTMS are often used as '*disruptive*' techniques to directly assess the causal role of a brain area in a given cognitive or perceptual process (Pascual-Leone, Walsh, & Rothwell, 2000), with sTMS being used as a method of disrupting these processes at a particular time point and rTMS being used as a method of prolonged disruption. Experimental use of both sTMS and rTMS has seen fruitful application in a variety of research areas such as motor function, language, vision, and attention (Hallett, 2007; Walsh & Cowey, 2000). RTMS has further utility as a clinical tool and has been used in the treatment of a number of psychological disorders (Kim, Pesiridou, & O'Reardon, 2009) and has shown further promise as a therapeutic technique for chronic pain, stroke rehabilitation, and epilepsy (Fregni & Pascual-Leone, 2007; Rossi & Rossini, 2004).

The study of TMS-evoked activity in the human brain has been approached by performing noninvasive neuroimaging in conjunction with TMS. A number of studies have examined the enduring plasticity-like effects of rTMS by administering rTMS prior to performing brain imaging (Ziemann, 2004). However, in this paper, we are concerned with the immediate effects of TMS and thus the simultaneous application of TMS and neuroimaging. We will use the term "concurrent" to refer to conditions in which the measures are taken at the same moment in which TMS pulses are delivered (for high-temporal resolution techniques such as EEG/ERP and EROS) or within a few seconds, using interleaved recording (as for hemodynamic-based techniques such as fMRI and PET). To date, both sTMS- and rTMS-evoked cortical activity has been measured successfully using a variety of noninvasive neuroimaging techniques, including EEG (sTMS: Ilmoniemi et al., 1997; for review see Ilmoniemi & Kičić, 2010), fMRI (rTMS: Bohning et al., 1998, 1999; see Bestmann et al., 2008 for review), PET (rTMS: Fox et al., 1997, 2006; Paus et al., 1997), and functional near-infrared spectroscopy (fNIRS; sTMS: Mochizuki, Ugawa, Terao, & Sakai, 2006).

Concurrent TMS/neuroimaging approaches also have broad appeal to the neurosciences as methods of mapping connectivity within the human brain (Paus, 2005). A TMS pulse does not solely activate a targeted brain area but interconnected regions as well (Baudewig et al., 2001; Bohning et al., 1999; Bestmann, Baudewig, Siebner, Rothwell, & Frahm, 2003, 2004). As such, it is possible to use TMS-locked activity to measure connectivity with the site of stimulation (see Bestmann et al., 2008 for review). Concurrent TMS/fMRI/PET has been

used to assess connectivity within the motor system (Baudewig et al., 2001; Bohning et al., 1999; Bestmann et al., 2003, 2004), visual system (Ruff et al., 2006, 2008), and prefrontal cortex (Speer et al., 2003). This approach provides an unprecedented method of assessing causal inter-regional connectivity in the human brain and may even be able to provide a metric for assessing the strength of connectivity between brain areas (Fox et al., 2006).

Neuroimaging methodologies used in conjunction with TMS suffer either from temporal or spatial limitations. FMRI and PET produce high quality spatial maps of TMS-induced activity but provide limited information regarding the timing of such activity. Conversely, EEG/ERP has millisecond temporal resolution but provides limited information about where the signal arises. Examining TMS-induced activity and inter-regional connectivity would benefit greatly from a technique with good temporal and spatial resolution. EROS may provide such an approach. EROS is a non-invasive optical imaging technique that uses near-infrared light to measure cortical activity (Gratton et al., 1995; Gratton & Fabiani, 2007, 2010). Electrical activity in the brain is associated with a synchronous change in the scattering of light, a phenomenon known as the fast optical signal (Rector et al., 1997, 2005). Specifically, active neural tissue exhibits less scattering, allowing photons to penetrate slightly deeper into the tissue. As a result, on average, it takes light longer to travel between a source and a detector when the cortex is active than when it is at rest. Thus, measuring the average delay of light between a near-infrared source and detector allows for the inference of activity in underlying neural tissue (see Gratton & Fabiani, 2009, 2010 for review). Because the fast optical signal occurs simultaneously with electrical activity, EROS is capable of very high temporal resolution. Additionally, the physical principles governing the movement of near-infrared light through the tissue give EROS a relatively high spatial resolution as well ($< 1.0\ cm^3$; Gratton & Fabiani, 2003).

Here, we use EROS to measure activity evoked in primary motor cortex by single-pulse TMS. The primary aims of this study were to establish 1) that EROS can be reliably measured in conjunction with TMS and 2) that EROS can be used to measure the time course of TMS-evoked cortical activity. Our study focused on the motor system as the majority of TMS/neuroimaging studies have focused on primary motor cortex (M1) and TMS-induced activity is best understood within this area (Chen, 2004; Di Lazzaro et al., 2004). Furthermore, M1 stimulation results in an overt distal muscle contraction (motor evoked potential, or MEP) that provides a method of assessing the effectiveness of cortical stimulation.

Method

Subjects

Nine right-handed participants (5 females, mean age = 23.1 years) took part in this study. All procedures were approved by the University of Illinois Institutional Review Board. Written informed consent was obtained from each participant prior to experimentation. All participants underwent extensive TMS safety screening in accordance with recommended procedures (Wasserman, 1998; Rossi et al., 2009).

Stimuli and Procedure

The present experiment focused on a subset of data obtained in a larger concurrent optical imaging and TMS study. In this study, participants performed a cued Go/NoGo task while TMS was randomly delivered on a subset of trials. The current analysis focuses on TMS pulses that were delivered during inter-trial intervals of this task. A 1250 ms fixation interval preceded each trial. On a random 20% of these fixation periods, single pulse TMS was delivered 750 ms into this inter-trial interval. Though TMS was given at other periods

during testing, inter-trial TMS pulses were the focus of this analysis as these are most appropriate for examining activity evoked in resting motor cortex.

Following placement of electromyographic (EMG) electrodes and TMS mapping of left and right hand representations (see *Transcranial Magnetic Stimulation* section below), participants were fitted with optical patches over the left and right hemispheres (Figure 1B). The participant's head was secured in a chin rest with forehead support and the TMS coil was held in position by the experimenter. Each participant was given 20 blocks, each containing 60 trials, a random twelve of which contained a TMS pulse. The coil was alternated between the two hemispheres every five blocks and the hemisphere to which TMS was delivered first was counterbalanced between subjects. A total of 120 pulses were delivered to each hemisphere. TMS pulses delivered to the left and right hemispheres will be referred to herein as the “TMS-LEFT” and “TMS-RIGHT” conditions, respectively.

Transcranial Magnetic Stimulation

TMS was delivered using a Magstim 200^2 monophasic stimulator (Magstim, Whitland, UK) with a double 70 mm coil (figure-of-eight coil). The M1 hand representation was localized by first centering the coil over the vertex and then moving the center of the coil ventrally in 1 cm steps until a visible contraction of the first dorsal interosseous (FDI) muscle was observed. Positions were mapped for the left and right hemispheres and optical patches were then centered on these locations. Patches were designed to allow the TMS coil to be positioned as close to scalp as possible but their use did introduce some additional distance between scalp and coil. We estimate this distance to be between 3 and 4 mm, on average. Following placement of optical patches and probes, approximate motor thresholds were determined by adjusting stimulator intensity in 5% increments until a visible contraction of the FDI muscle was observed. Thresholds were determined independently for the left and right hemispheres. The intensity determined by the highest threshold was then applied to both hemispheres during testing. The mean level of stimulator output, across subjects, was approximately 80% of the maximum output. All functional mapping and experimental testing were conducted with the figure-of-eight coil in a posterior-to-anterior orientation.

MEPs

EMG was recorded from the FDI muscle of the hand contralateral to the figure-of-eight coil. EMG was amplified with an EMG100C (BIOPAC, Goletta, CA). Data were bandpass-filtered online 1.0 – 500 Hz, digitized at 5000 Hz, and recorded with custom software written in Labview (National Instruments, Austin, Texas, USA). Offline, MEPs were calculated by averaging epochs (-20 ms to 100 ms) time-locked to the occurrence of the TMS pulse. Prior to averaging, each epoch was baseline-corrected according to the 20-ms pre-stimulus interval and rectified by taking the absolute value of each data point within the epoch. MEP amplitude was quantified as the mean rectified activity between 28 and 30 ms.

EROS Recording and Analysis

In order to simultaneously record EROS from beneath a figure-of-eight coil, low-profile optical “patches” were constructed such that near-infrared sources and detectors could make contact with exposed scalp while still allowing the TMS coil to be positioned close enough to the cortex to elicit an MEP. Two flat rubber patches (one for each hemisphere) were constructed and each mounted with four silvered prisms. Prisms enabled thick detector fibers (3.0 mm diameter) to be attached such that they rested flush against the head (Figure 1A) rather than perpendicular to it, as is typical for most EROS experiments. Smaller source fibers (0.4 mm diameter) were inserted into the patch through small angled holes. A small window in the center of the apparatus allowed the patch to be centered directly over the TMS-mapped location of the M1 hand representation and allowed the coil to make closer

contact with the scalp. Before mounting optical patches, participants' hair was diligently parted and secured to ensure that all detectors were positioned over exposed scalp.

Each patch consisted of a column of four detectors and four source fibers, separated by a distance of approximately 4.0 cm. A fifth source fiber was positioned approximately 1.0 cm from the dorsal-most detector. It is known that, at long distances (3 – 5 cm), light penetrates relatively deeply into the head (1 – 3 cm; Gratton & Fabiani, 2010). However, at short distances (< 1.5 cm), light takes a very superficial path between source and detector and does not pass through the cortex. This short distance source-detector pair was included to rule out TMS-evoked optical responses as being anything but cortical in origin (for a similar approach see Medvedev, Kainerstorfer, Borisov, Barbour, & VanMeter, 2009). If EROS activations were not of cortical origin (e.g., movement and muscle artifacts, electrical artifact, or change in skin reflectance) then short channels should show a similar pattern of results to that of the long channels. In contrast, EROS of cortical origin should be apparent only in long channels. The digitized positions of source and detector fibers are overlaid on a representative subject's rendered structural MRI in Figure 1C.

Optical recordings were taken using four modified frequency-domain oxymeters (model 96208, ISS, Champaign, IL). The recording montage consisted of two of the previously described optical patches, one centered over the left motor cortex and one over the right. Source fibers emitted near-infrared light at a wavelength of 830 nm, modulated at 110 MHz. Phase-delay optical data were sampled from each source-detector pair (total of 40 channels) at a rate of 125 Hz (8 ms samples). It should be noted that the multiplexing of sources occurs over the entirety of the 8 ms sample interval. Thus, sampling began every 8 ms but did not complete until the end of the 8 ms sample interval. As such, a given sample represents activity over an 8 ms period. Timing will herein be reported from the beginning of a given sampling interval (e.g., timing of 8 ms represents a measurement taken between 8 and 16 ms, when the next sampling interval begins).

During the optical session, detector and source locations for each participant were digitized in three-dimensional space using a Polhemus 3 Space digitizer (Colchester, VT, USA). Three fiducial points (nasion, left and right pre-auricular points) and a number of additional points outlining the head shape were also digitized and used for offline co-registration of optical data to a structural T1-weighted MRI obtained in a separate session. Co-registration was performed with a custom fitting algorithm (Whalen, Maclin, Fabiani, & Gratton, 2008) implemented in Matlab (Mathworks, Natick, MA, USA). This co-registration procedure has been shown to substantially improve the spatial resolution and quality of EROS signals. In this study, optical fibers were centered on TMS-mapped hand representations. As such, optical data were already functionally aligned to M1 for each individual subject. The three-dimensional reconstruction of the optical data was achieved on the basis of a co-registration of a single representative subject into Talairach space. This did not change the correspondence of each subject's map with the point stimulated by TMS.

EROS data were pre-processed using custom software written in Matlab. Pre-processing consisted of phase wrapping correction, conversion of angular phase to a delay measure (picoseconds), pulse correction (Gratton & Corballis, 1995), and 30 Hz low-pass filtering. Phase delay data were then segmented into epochs time-locked to the onset of TMS pulses (-72 ms to +500 ms) and averaged together separately for TMS-LEFT and TMS-RIGHT conditions. For further information on each of these processing steps refer to Gratton and Fabiani (2007, Gratton and Fabiani 2010).

Long-distance source-detector channels were analyzed using a custom software package, OPT-3D (Gratton, 2000). This program is used to model mean diffusion paths between

source-detector pairs in Talairach space and to perform group-level statistics. Source-detector channels that fell outside of a 2.0 – 5.5 cm range were excluded from analysis as were channels in which standard deviation of the delay measure exceeded 80 picoseconds. A 6.0 mm spatial Gaussian filter was applied to Talairach-transformed data. Phase delay data were baseline corrected according to a 72 ms pre-stimulus interval. Group-level *t*-statistics were calculated for each voxel, then converted to *z*-scores. Thresholded activation maps were then surface-projected onto a superior view of a template Talairach brain. All statistical analyses are based on these surface-projected maps. Two 4.5 cm × 1.5 cm (width × height) regions of interest (ROIs) covering Brodmann area 4 were used for statistical analysis of TMS-evoked activity in left and right hemispheres. ROI placement and dimensions were based on TMS mapping, areas of optical coverage, and known anatomical coordinates of motor cortex. The left hemisphere ROI was from x=-62 to x=-17 and from y=-20 to y=-5. The right hemisphere ROI was from x=5 to x=50 and from y=-20 to y=-5. Note that these ROIs do not contain a z-dimension as the data are derived from surface axial projection onto a template Talairach brain. Left and right hemisphere ROIs were analyzed for both TMS-LEFT and TMS-RIGHT conditions. Correction for multiple comparisons within an ROI was conducted using a method based on the number of independent resolution elements within the boundaries of the ROI (Friston et al., 1994; Gratton et al., 2006).

Analysis of short-distance channels was conducted by collapsing together the short-channels ipsilateral to the TMS coil for each subject, computing *t*-statistics across the entire time course, and then converting these to z-scores. A critical z of 1.96 was used to evaluate statistical significance.

Results

MEPs

MEPs exhibited typical onset latency and amplitude (Figure 2). Mean amplitude was 300.7 μV (SE=49.7 μV) for the right FDI and 212.1 μV (SE=55.4 μV) for left FDI. MEPs clearly demonstrate that the coil's magnetic field was able to stimulate primary motor cortex even with the optical patch mounted between the coil and scalp.

EROS

Figure 3 shows the time course of the fast optical response over the 64 ms period following TMS onset. Activation maps are shown separately for TMS-LEFT and TMS-RIGHT conditions. TMS-LEFT showed initial activation in left motor cortex (ipsilateral to coil position) followed by activation in the right motor cortex (contralateral to coil). Left hemisphere EROS activity achieved statistical significance at 16 and 24 ms following the TMS pulse onset (16 ms peak $z = 2.35$, $z_{crit} = 2.34$, x = -43, y = -11; 24 ms peak $z = 2.33$, $z_{crit} = 2.30$, x = -43, y = -11). Significant activations in the TMS-LEFT conditions then occurred in the contralateral (right) hemisphere ROI, achieving statistical significance from 40 to 48 ms post-TMS (40 ms peak $z = 2.64$, $z_{crit} = 2.19$, x = 42, y = -21; 48 ms peak $z = 2.76$, $z_{crit} = 2.27$, x = 39, y = -21). TMS-RIGHT showed only early EROS activity in the right hemisphere ROI. TMS-locked activity in the right hemisphere was statistically reliable at 16 and 24 ms (16 ms peak $z = 2.93$, $z_{crit} = 2.46$, x = 7, y = -6; 24 ms peak $z = 2.65$, $z_{crit} = 2.33$, x = 7, y = -8). No contralateral (left) hemisphere activity was apparent in the TMS-RIGHT condition.

Peak ipsilateral activation waveforms are given in Figure 4. The time window of interest for this experiment comprised the initial 64 ms following the pulse and shows a clear peak in response to TMS onset. For thoroughness, Figure 4 also plots EROS activity over an extended 500 ms time window. Later EROS data shows oscillatory activity in the beta band

(14-35 Hz). Further work is necessary to characterize these oscillations as it not clear whether these patterns reflect only TMS-induced activity or have contributions from endogenous beta due to preparation for the upcoming manual response task.

An additional control analysis examined short distance channels (1.0 cm) for TMS-locked EROS activity. Light from such short-distance channels only penetrates superficially into the head and will not pass through cortex. Short-distance channels revealed no significant EROS activations in response to ipsilateral TMS pulses. The time course of short-distance channel activity is plotted against peak ipsilateral activations for long-distance channels in Figure 4.

We further sought to provide an estimate of the area of local cortical tissue activated by the TMS pulse. To provide such an estimate we used the 16 ms time point with the rationale that at such short latency the response was not likely to have spread to secondary areas. We calculated all pixels that exceeded a *z*-value of 2.0 and were contiguous with the peak activation, irrespective of whether they extended beyond the ROI used to initially establish the peak. Using these parameters, ipsilateral activation in the TMS-LEFT and TMS-RIGHT conditions was present over areas of 4.2 cm^2 and 1.7 cm^2, respectively. In our recordings we can estimate the spatial resolution using a resel size approach (Friston et al., 1994), and resel size was of the order of 0.5-1.0 cm^2. This indicates that the area activated by the TMS pulse was substantially larger than a resel. It is important to note, however, that a number of factors contribute to the spatial resolution of EROS (e.g., source-detector density, inter-subject variability, spatial filtering parameters; Gratton & Fabiani, 2010). Thus, the estimates of spatial spread provided here are relative to the current recording parameters and are likely to vary as a function of recording montage and pulse strength.

Discussion

This study examined TMS-induced activity in human motor cortex using EROS, a fast optical imaging method sensitive to instantaneous changes in neural activity. Using EROS, we were able to track the evolution of TMS-induced activity in left and right motor cortex. Robust cortical activation was apparent directly beneath the stimulating coil (M1) at 16 ms post-pulse and, for left hemisphere stimulation, shifted to the contralateral hemisphere within 40 ms. Several aspects of the data indicate that the effects of TMS were cortical in nature. First, some of the activity was observed at a time (40 ms after the coil discharged) and location (i.e., the contralateral hemisphere) distant from the coil. Second, and more importantly, EROS activity cannot be explained by a non-cortical origin as effects were present only in long-distance channels (2.0 – 5.5 cm) but not short-distance channels (1.0 cm), the light from which does not penetrate deep enough to pass through cortex.

Early ipsilateral TMS-locked EROS activity is consistent with a number of previous neuroimaging studies. FMRI and PET studies have reported local activations in M1 hand representations, occurring directly beneath the coil with suprathreshold stimulation (Baudewig et al., 2001; Bestmann et al., 2003, 2004; Bohning et al., 1998, 1999; Fox et al., 1997, 2006; Paus et al., 1997). It is difficult to draw a direct comparison between the current TMS/EROS results and those of fMRI or PET as the nature of signals between these methodologies is qualitatively different (i.e., neuronal versus hemodynamic), the temporal scale varies by several orders of magnitude, and concurrent TMS/fMRI/PET studies have used rTMS (as opposed to the sTMS used here). Despite these methodological disparities short-latency EROS results align well with other neuroimaging studies. The current EROS results demonstrate that, within 16 ms of pulse onset, ipsilateral TMS-evoked activity can also be localized to M1 hand representations. Furthermore, this early activation appears to exhibit a local spread comparable to that described in concurrent TMS/fMRI studies of

motor cortex (e.g., Bohning et al., 1999). Future optical imaging studies using multiple wavelengths could simultaneously record the fast optical signal and the slow fNIRS hemodynamic response to directly compare the spatial spread of a TMS pulse as quantified by these two measures.

A later contralateral TMS-evoked activation (40 ms) was also apparent for left hemisphere stimulation. Given the time course of this contralateral activation we presume this activity to be trans-synaptic propagation of TMS-evoked activity either subcortically or via the corpus callosum (Ilmoniemi et al., 1997). It is unclear why this contralateral activity was significant for left and not right hemisphere TMS, but it may be due, in part, to the use of the same level of stimulator output for both hemispheres. Left M1 is typically more sensitive to TMS than right M1 for right-handed individuals (Triggs, Calvanio, Macdonell, Cros, & Chiappa, 1994). As such, pulses delivered to the left hemisphere may have induced a more robust contralateral response than those delivered to the right. If this explanation is verified, it implies that more intense stimulation allows for the signal to propagate more distally than when the stimulation is less intense. However, additional controls are necessary to completely understand the source of this contralateral activation and its apparent hemispheric asymmetry.

The use of EROS concurrently with TMS allowed TMS-evoked cortical activity to be investigated with unprecedented temporal and spatial resolution, giving EROS a unique advantage over other neuroimaging techniques. Simultaneous TMS/fMRI and TMS/PET studies have demonstrated robust TMS-evoked activations on a fine spatial scale (Bestmann et al., 2008; Paus, 2005). However, the sluggishness of hemodynamic/metabolic responses prohibit the use of these techniques for the investigation of the temporal dynamics induced by a single TMS pulse and limits the types of questions that can be addressed with this technique. For example, TMS/fMRI studies in motor cortex cannot unambiguously differentiate activations induced in M1 by a suprathreshold TMS pulse from those due to afferent muscle feedback from the resultant MEP (Baudewig et al., 2001; Bestmann et al., 2003; Bohning et al., 1999). Simultaneous TMS/EROS measurements do not suffer from such a temporal ambiguity. Our results show activations ipsilateral to coil position starting immediately after the pulse and peaking at 16 ms latency, several milliseconds before an MEP was even measurable. Therefore, we can rule out that this EROS activity is due to re-afferent feedback, which can be expected to have a latency of at least 50-60 ms.

Simultaneous TMS/ERP recordings have the converse problem to that of TMS/fMRI recordings. TMS-locked ERP studies identified a number of positive and negative deflections occurring over several hundred milliseconds after a TMS pulse, but the cortical origin of these components is unclear (Bonato, Miniussi, & Rossini, 2006; Ilmoniemi et al., 1997). TMS/EROS was able to resolve TMS-locked activity on a temporal scale comparable to that of ERPs (125 Hz sampling rate in the present experiment) but was able to disambiguate the cortical locus of this activity as well. TMS/EROS results clearly showed initial activity in ipsilateral M1, followed shortly thereafter by contralateral M1 activity (at least in the case of left hemisphere TMS).

An additional advantage of using EROS in conjunction with TMS is that it is not susceptible to the same magnetic field artifacts that can affect ERP or fMRI acquisition. TMS/EEG studies are often incapable of recording the initial few milliseconds following a pulse due to the sample-and-hold circuits used to prevent amplifier saturation. TMS/fMRI experiments require scans to be interleaved with TMS pulses with a delay of about 100 ms to avoid magnetic field distortion. EROS measurements are based on the passage of near-infrared light through the head rather than measurements of electrical or magnetic fields. Thus, EROS can provide continuous, uninterrupted acquisition during a TMS pulse.

A recent review by Ilmoniemi and Kičić (2010) described several sources of artifact for concurrent TMS/EEG recordings in addition to the magnetic artifact. As some of these artifacts could potentially apply to optical recordings as well, a subset of these artifacts deserve discussion in the context of EROS. A TMS pulse can activate muscle tissue on the scalp in addition to the underlying cortical tissue. Since near-infrared light must pass through scalp tissue, such time-locked muscle activity could be a potential source of artifact for EROS recordings and may appear as a false cortical activation. Though little muscle tissue is present on the regions of scalp stimulated in this experiment, muscle artifact cannot be ruled out on this basis alone. The inclusion of a short distance optical channel allowed us to assess the contribution of muscle activity to EROS activations. Light from a short-distance channel penetrates only superficially (~5 mm) into scalp and skull, allowing the contribution of muscle artifact to be evaluated independently of cortical activations. As no short-channel activations were found, major muscle artifact can be ruled out.

Another potential source of artifact arises from movement and vibration of the coil upon discharge of the magnetic field, which could result in the displacement of optical source fibers. Again, the inclusion of a short-distance channel allows for the presence of such an artifact to be assessed. We found no evidence of time-locked movement artifact in this experiment. The fact that a second delayed activation was observed contralateral to the coil also speaks against a movement artifact.

A final possible artifact arises from auditory stimulation due to coil ‘clicking’ and somatic stimulation of the scalp from magnetic and mechanical stimulation. Eliminating the occurrence of sensory artifacts is difficult. However, the temporal and spatial resolution of EROS makes this technique less prone to misinterpretations of these artifacts. TMS-evoked EROS signals have a clear cortical source and an unambiguous time course and make it possible, to an extent, to disentangle TMS-induced activations from those resulting from non-TMS sources. In this experiment, initial ipsilateral TMS-evoked activations are clearly due to magnetic stimulation as the latency of these signals is too short to be the result of sensory stimulation or feedback, which is expected to exceed 20 ms. Furthermore, EROS signals were measured from motor cortex ROIs, which clearly rules out an auditory component and, to a lesser extent, somatosensory stimulation.

Though TMS/EROS provides a method of temporally and spatially tracking a TMS-locked response, the technique has several limitations relative to other neuroimaging methodologies. First, EROS is only capable of measuring signals from the cortical surface (Gratton & Fabiani, 2010) and cannot be used to investigate activations of medial temporal cortex or deep subcortical structures. Though subcortical structures cannot be directly stimulated with surface-coil TMS, surface stimulation could result in indirect trans-synaptic activations of subcortical areas but such activations would remain invisible to EROS. In addition, the signal-to-noise ratio of EROS is quite low compared to other neuroimaging methodologies and necessitates the collection of many trials, which may limit the types of questions that can be addressed using this approach. However, it should be noted that, in this study, TMS-evoked EROS signals were approximately three times as large as those typically recorded in EROS experiments, indicating that signal-to-noise may be less of an issue when signals are evoked exogenously with TMS.

Conclusions

Our results indicate that concurrent TMS/EROS shows great promise as a tool to investigate the dynamics of TMS-induced activity in human cortex. This approach can further the understanding of TMS mechanisms in the human brain and could be easily adapted for use with other methods of brain stimulation as well (i.e., transcranial direct current stimulation,

tDCS). Though the present examination focused only on activity within the left and right motor strips, with further development, TMS/EROS could be used to explore cortico-cortical connectivity more extensively by investigating neural systems beyond motor cortex and adding more optical channels for greater head coverage.

Acknowledgments

This was supported by NIMH grant R01-80182 to G. Gratton, and by a Beckman Institute Postdoctoral Fellowship to Nathan Parks.

References

Baudewig J, Siebner HR, Bestmann S, Tergau F, Tings T, Paulus W, Frahm J. Functional MRI of cortical activations induced by transcranial magnetic stimulation (TMS). Neuroreport. 2001; 12:3543–3548. [PubMed: 11733708]

Bestmann S, Baudewig J, Siebner HR, Rothwell JC, Frahm J. Subthreshold high-frequency TMS of human primary motor cortex modulates interconnected frontal motor areas as detected by interleaved fMRI-TMS. Neuroimage. 2003; 20:1685–1696. [PubMed: 14642478]

Bestmann S, Baudewig J, Siebner HR, Rothwell JC, Frahm J. Functional MRI of the immediate impact of transcranial magnetic stimulation on cortical and subcortical motor circuits. European Journal of Neuroscience. 2004; 19:1950–1962. [PubMed: 15078569]

Bestmann S, Ruff CC, Blankenburg F, Weiskpf N, Driver J, Rothwell JC. Mapping causal interregional influences with concurrent TMS-fMRI. Experimental Brain Research. 2008; 191:383–402.

Bohning DE, Shastri A, McConnell KA, Nahas Z, Lorberbaum JP, Roberts DR, Teneback C, Vincent DJ, George MS. A combined TMS/fMRI study of intensity-dependent TMS over motor cortex. Biological Psychiatry. 1999; 45:385–394. [PubMed: 10071706]

Bohning DE, Shastri A, Nahas Z, Lorberbaum JP, Andersen SW, Dannels WR, Haxthausen EU, Vincent DJ, George MS. Echoplanar BOLD fMRI of brain activation induced by concurrent transcranial magnetic stimulation. Investigative Radiology. 1998; 33:336–340. [PubMed: 9647445]

Bonato C, Miniussi C, Rossini PM. Transcranial magnetic stimulation and cortical evoked potentials: a TMS/EEG co-registration study. Clinical Neurophysiology. 2006; 117:1699–1707. [PubMed: 16797232]

Chen R. Interactions between inhibitory and excitatory circuits in the human motor cortex. Experimental Brain Research. 2004; 154:1–10.

Di Lazzaro V, Oliviero A, Pilato F, Saturno E, Dileone M, Mazzone P, Insola A, Tonali PA, Rothwell JC. The physiological basis of transcranial motor cortex stimulation in conscious humans. Clinical Neurophysiology. 2004; 115:255–266. [PubMed: 14744565]

Fox P, Ingham R, George MS, Mayberg H, Ingham J, Roby J, Martin C, Jerabek P. Imaging human intra-cerebral connectivity by PET during TMS. Neuroreport. 1997; 8:2787–2791. [PubMed: 9295118]

Fox PT, Narayana S, Tandon N, Fox SP, Sandoval H, Kochunov P, Capaday C, Lancaster JL. Intensity modulation of TMS-induced cortical excitation: primary motor cortex. Human Brain Mapping. 2006; 27:478–487. [PubMed: 16161021]

Fregni F, Pascual-Leone A. Technology insight: noninvasive brain stimulation in neurology-perspectives on the therapeutic potential of rTMS and tDCS. Nature Clinical Practice Neurology. 2007; 3:383–393.

Friston KJ, Holmes AP, Worsley KJ, Poline JP, Frith CD, Frackowiak RSJ. Statistical parametric maps in functional imaging: a general linear approach. Human Brain Mapping. 1994; 2:189–210.

Gratton G. “Opt-cont” and “opt-3D”: a software suite for the analysis and 3D reconstruction of the event-related optical signal (EROS). Psychophysiology. 2000; 37:S44–S144.

Gratton G, Brumback CR, Gordon BA, Pearson MA, Low KA, Fabiani M. Effects of measurement method, wavelength, and source-detector distance on the fast optical signal. Neuroimage. 2006; 32:1576–1590. [PubMed: 16872842]

Gratton G, Corballis PM. Removing the heart from the brain – compensation for the pulse artifact in the photon migration signal. Psychophysiology. 1995; 32:292–299. [PubMed: 7784538]

Gratton G, Corballis PM, Cho E, Fabiani M, Hood DC. Shades of gray matter: noninvasive optical images of human brain responses during visual stimulation. Psychophysiology. 1995; 32:505–509. [PubMed: 7568645]

Gratton G, Fabiani M. The event-related optical signal (EROS) in visual cortex: replicability, consistency, localization, and resolution. Psychophysiology. 2003; 40:561–571. [PubMed: 14570164]

Gratton, G.; Fabiani, M. Optical imaging. In: Parasuraman, R.; Rizzo, M., editors. Neuroergonomics: The Brain at Work. Oxford University Press; Cambridge, MA: 2007. p. 65-81.

Gratton G, Fabiani M. Fast optical imaging of human brain function. Front Hum Neurosci. 2010; 4:52. [PubMed: 20631845]

Hallett M. Transcranial magnetic stimulation: a primer. Neuron. 2007; 55:187–199. [PubMed: 17640522]

Huang YZ, Edwards MJ, Rounis E, Bhatia KP, Rothwell JC. Theta burst stimulation of the human motor cortex. Neuron. 2005; 45:201–206. [PubMed: 15664172]

Ilmoniemi RJ, Kičić D. Methodology for combined TMS and EEG. Brain Topography. 2010; 22:233–248. [PubMed: 20012350]

Ilmoniemi RJ, Virtanen J, Ruohonen J, Karhu J, Aronen HJ, Näätänen R, Katila T. Neuronal responses to magnetic stimulation reveal cortical reactivity and connectivity. Neuroreport. 1997; 10:3537–3540. [PubMed: 9427322]

Kim DR, Pesiridou A, O'Reardon JP. Transcranial magnetic stimulation in the treatment of psychiatric disorders. Current Psychiatry Reports. 2009; 11:447–452. [PubMed: 19909666]

Medvedev AV, Kanerstorfer J, Borisov SV, Barbour RL, VanMeter J. Event-related optical signal in a rapid object recognition task: improving detection by the independent component analysis. Brain Research. 2008; 1236:145–158. [PubMed: 18725213]

Mochizuki H, Ugawa Y, Terao Y, Sakai KL. Cortical hemoglobin-concentration changes under the coil induced by single-pulse TMS in humans: a simultaneous recording with near-infrared spectroscopy. Experimental Brain Research. 2006; 169:302–310.

Pascual-Leone A, Walsh V, Rothwell J. Transcranial magnetic stimulation in cognitive neuroscience – virtual lesion, chronometry, and functional connectivity. Current Opinion in Neurobiology. 2000; 10:232–237. [PubMed: 10753803]

Paus T. Inferring causality in brain images: a perturbation approach. Philosophical Transactions of the Royal Society of London, Series B, Biological Sciences. 2005; 360:1109–1114.

Paus T, Jech R, Thompson CJ, Comeau R, Peters T, Evans AC. Transcranial magnetic stimulation during positron emission tomography: a new method for studying connectivity of the human cerebral cortex. Journal of Neuroscience. 1997; 17:3178–3184. [PubMed: 9096152]

Rector DM, Carter KM, Volegov PL, George JS. Spatio-temporal mapping of rat whisker barrels with fast scattered light signals. Neuroimage. 2005; 26:619–627. [PubMed: 15907319]

Rector DM, Poe GR, Kristensen MP, Harper RM. Light-scattering changes follow evoked potentials from hippocampal Schaeffer collateral stimulation. Journal of Neurophysiology. 1997; 78:1707–1713. [PubMed: 9310454]

Ridding MC, Rothwell JC. Is there a future for therapeutic use of transcranial magnetic stimulation? Nature Reviews Neuroscience. 2007; 8:559–567.

Rossi S, Hallett M, Rossini PM, Pascual-Leone A, Avanzini G, Bestmann S, et al. Ziemann U. Safety, ethical considerations, and application guidelines for the use of transcranial magnetic stimulation in clinical practice and research. Clinical Neurophysiology. 2009; 120:2008–2039. [PubMed: 19833552]

Rossi S, Rossini PM. TMS in cognitive plasticity and the potential for rehabilitation. Trends in Cognitive Sciences. 2004; 8:273–279. [PubMed: 15165553]

Triggs WJ, Calvanio R, Macdonell RAL, Cros D, Chiappa KH. Physiological motor asymmetry in human handedness: evidence from transcranial magnetic stimulation. Brain Research. 1994; 636:270–276. [PubMed: 8012811]

Walsh V, Cowey A. Transcranial magnetic stimulation and cognitive neuroscience. Nature Reviews Neuroscience. 2000; 1:73–79.

Wasserman EM. Risk and safety of repetitive transcranial magnetic stimulation: report and suggested guidelines from the International Workshop on the Safety of Repetitive Transcranial Magnetic Stimulation. Electroencephalography and Clinical Neurophysiology. 1998; 108:1–16. [PubMed: 9474057]

Ruff CC, Bestmann S, Blankenburg F, Bjoertomt O, Josephs O, Weiskopf N, Deichmann R, Driver J. Distinct causal influences of parietal versus frontal areas on human visual cortex: evidence from concurrent TMS-fMRI. Cerebral Cortex. 2008; 18:817–827. [PubMed: 17652468]

Ruff CC, Blankenburg F, Bjoertomt O, Bestmann S, Freeman E, Haynes JD, Rees G, Josephs O, Deichmann R, Driver J. Concurrent TMS–fMRI and psychophysics reveal frontal influences on human retinotopic visual cortex. Current Biology. 2006; 16:1479–1488. [PubMed: 16890523]

Speer AM, Willis MW, Herscovitch P, Daube-Witherspoon M, Shelton JR, Benson BE, Post RM, Wassermann EM. Intensity-dependent regional cerebral blood flow during 1-Hz repetitive transcranial magnetic stimulation (rTMS) in healthy volunteers studied with H215O positron emission tomography: II. Effects of prefrontal cortex rTMS. Biological Psychiatry. 2003; 54:826–832. [PubMed: 14550682]

Talairach, J.; Tournoux, P. A Co-planar Stereotaxic Atlas of a Human Brain. Thieme; Stuttgart: 1988.

Whalen C, Maclin EL, Fabiani M, Gratton G. Validation of a method for coregistering scalp recording locations with 3D structural MR images. Human Brain Mapping. 2008; 29:1288–1301. [PubMed: 17894391]

Ziemann U. TMS induced plasticity in human cortex. Reviews in Neurosciences. 2004; 15:253–266.

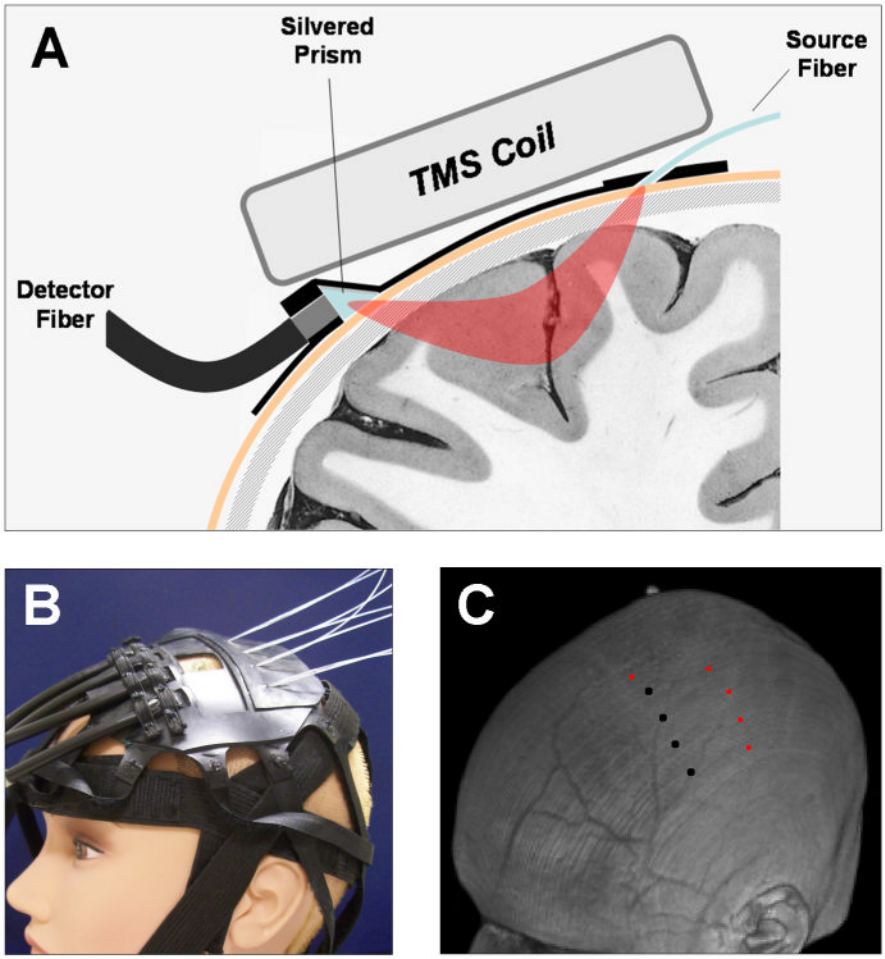

Figure 1.

(A) Optical patches for simultaneous EROS and TMS were constructed such that detector fibers were mounted against silvered prisms to maintain a low profile, allowing cortex to be stimulated by TMS. (B) Patches were constructed of flexible rubber and were fastened to the head using an elastic harness. (C) 3D reconstruction of left hemisphere source and detector locations for a representative subject. Detectors are represented by black dots and sources by red dots. Note the position of the most dorsal source that forms the short distance source-detector channel with the most proximal detector.

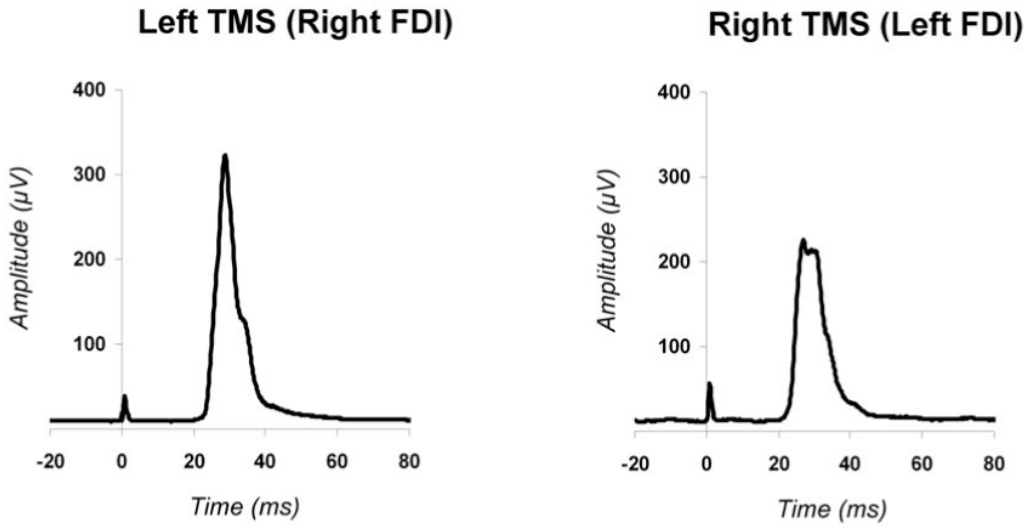

Figure 2.
Motor-evoked potentials elicited from TMS administered to left and right motor cortex.

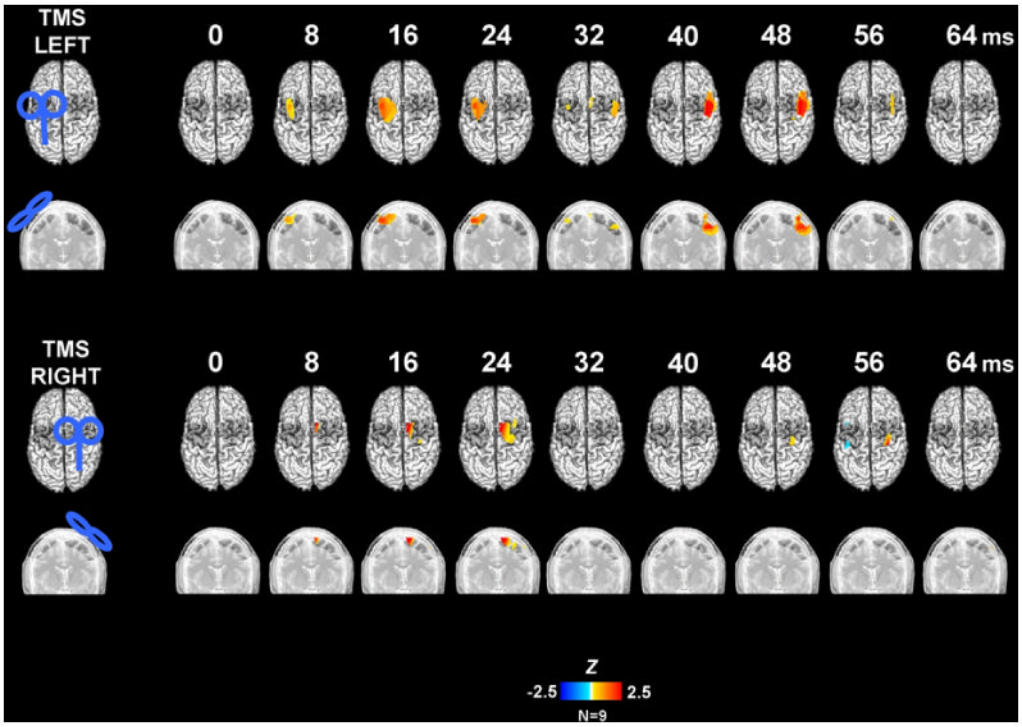

Figure 3.
Time course of TMS-evoked EROS response for left and right hemisphere stimulation. Axial views are surface-projected activation maps projected on a template brain (with skin and skull removed to facilitate visualization. Coronal views are taken from a representative slice (y=-10 for TMS-LEFT and y=3 for TMS-RIGHT). For these views, skin and skull were left in the image to demonstrate where the region of activation occurs in 3-D view. The dark grey regions represent the area sampled by the recording montage.

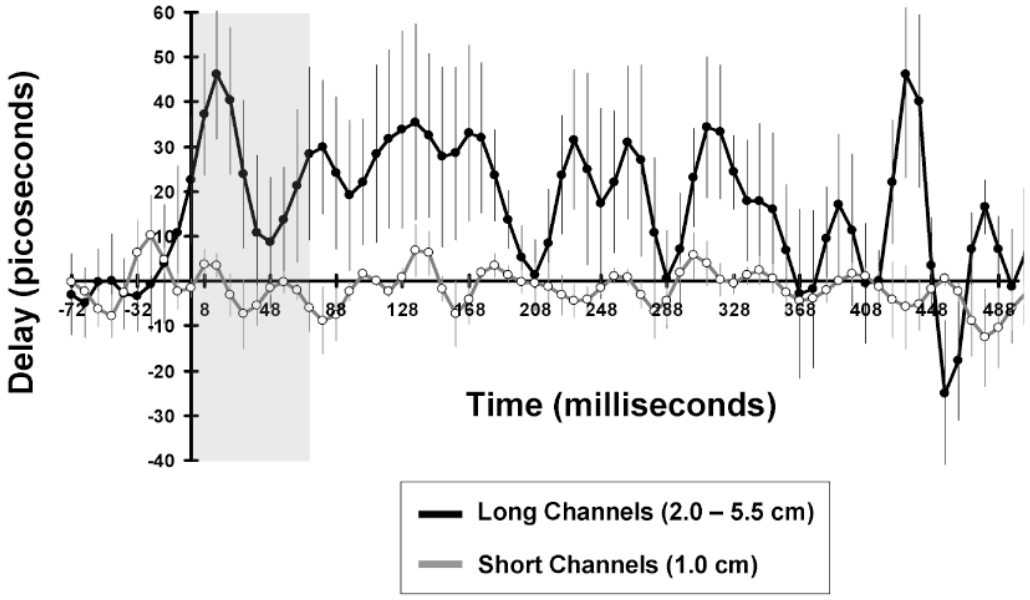

Figure 4.

Average waveforms of TMS-evoked EROS response for long and short channels. Averages from long channels are derived from the peak voxel in the grand average. Long- and short-channel waveforms are shown ipsilateral to TMS stimulation and are collapsed across TMS-LEFT and TMS-RIGHT conditions. A strong TMS-evoked response is evident in long-distance channels but absent in short-distance channels, demonstrating that the patterns of activation are cortical in origin. The highlighted time window indicates the primary focus of the study and the window over which the peak activity was determined. The time-course of long-distance channels shows an initial transient response to the TMS over the initial 32 ms followed by a more extended period of oscillatory activity for the remainder of the epoch. Note that, due to the use of a 30 Hz low-pass filter, activity in the long-channel plot appears to extend before time zero. Error bars indicate SE of the mean computed across subjects.